### SANDIA FRACTURE CHALLENGE 2017



# The third Sandia Fracture Challenge: from theory to practice in a classroom setting

Ashley D. Spear · Michael W. Czabaj · Pania Newell · Karen DeMille · Brian R. Phung · Dongfang Zhao · Peter Creveling · Nathan Briggs · Eric Brodbine · Christopher Creveling · Eric Edelman · Kristoffer Matheson · Caitlin M. Arndt · Megan Buelte · Stuart Childs · Isaac Nelson · Faramarz Safazadeh · Jordan French · Clay Audd · Austin J. Smith · Edward J. Dorrian · Gregory Clark · Jonathan Tayler · Renan Ichi

Received: 24 October 2018 / Accepted: 18 May 2019 / Published online: 25 June 2019 © Springer Nature B.V. 2019

**Abstract** Three computational methods for modeling fracture are compared in the context of a class' participation in the Third Sandia Fracture Challenge (SFC3). The SFC3 was issued to assess blind predictions of ductile fracture in a complex specimen geometry produced via additive manufacturing of stainless steel 316L powder. In this work, three finite-element-based methods are investigated: (1) adaptive remeshing, with or without material-state mapping; (2) element deletion; and (3) the extended finite element method. Each student team was tasked with learning about its respective method, calibrating model parameters, and performing blind prediction(s) of fracture/failure in the challengegeometry specimen. Out of 21 teams who participated in the SFC3, three of the seven student teams from this class project ranked among the top five based on either global force-displacement or local strain predictions. Advantages and disadvantages of the three modeling approaches are identified in terms of mesh dependency, user-friendliness, and accuracy compared to experimental results. Recommendations regarding project management and organization are offered to facilitate future classroom participation in the Sandia Fracture Challenge or similar blind round-robin exercises.

**Keywords** Computational fracture mechanics · Fracture · Tearing · Plasticity · Crack-growth simulation · Finite-element modeling

#### 1 Introduction

The Sandia Fracture Challenge (SFC), hosted by Sandia National Laboratories, is a well-established, international round-robin exercise designed to assess computational approaches for predicting ductile fracture. Each SFC relies on volunteer participants from around the world to submit blind predictions of ductile fracture for a non-trivial challenge scenario. In the first SFC (Boyce et al. 2014), 13 teams participated, and the teams were asked to predict failure path and load versus crack-opening displacement in a specimen geometry that was designed such that different failure paths were possible. Both the challenge-geometry and calibration specimens were made of 15-5 PH stainless steel. One of many important findings from the first SFC was that geometric uncertainties impacted the predictions of crack-path tremendously. In the second SFC (Boyce et al. 2016), 14 teams participated, and the teams were asked to predict global forces, crack-opening displacements, and crack path for a Ti-6Al-4V sheet of relatively complex geometry under quasi-static and modest-rate dynamic loading. While the second SFC

E. J. Dorrian · G. Clark · J. Tayler · R. Ichi University of Utah, Salt Lake City, USA

e-mail: ashley.spear@utah.edu



A. D. Spear ( $\boxtimes$ ) · M. W. Czabaj · P. Newell · K. DeMille ·

B. R. Phung  $\cdot$  D. Zhao  $\cdot$  P. Creveling  $\cdot$  N. Briggs  $\cdot$ 

E. Brodbine · C. Creveling · E. Edelman · K. Matheson ·

C. M. Arndt · M. Buelte · S. Childs · I. Nelson ·

F. Safazadeh · J. French · C. Audd · A. J. Smith ·

r. Sarazaden · J. French · C. Audu · A. J. Siliul

showed some improvements in predictions over the first SFC, new sources of discrepancies emerged. For example, one of many outcomes revealed through the second SFC was that inaccurate treatment of boundary conditions had a significant and negative impact on the fracture predictions. The third SFC, or SFC3, Kramer et al. (2019) was issued in 2017 and challenged teams to predict ductile fracture in additively manufactured 316L stainless steel tensile specimens containing a complex arrangement of internal cavities and channels. A total of 21 teams participated in the SFC3. Seven of the teams were from the University of Utah and participated in the SFC3 as a class project, marking the first time that an entire class has participated in any of the SFCs. The purpose of this manuscript is to describe—from both technical and organizational standpoints—the experience and results from the University of Utah teams' participation in the SFC3.

The participants from the University of Utah were graduate students enrolled in an upper-level graduate course entitled "Fatigue and Fracture", which is offered nominally every other year through the Department of Mechanical Engineering. In general, the course introduces students to theory and application of fracture mechanics and fatigue concepts. The course offering during the spring semester of 2017 happened to coincide with the issuance of the SFC3. During that semester, 20 students were enrolled in the course, all of whom participated in the project. Of the 20 students, all but three had previously taken a course on the finite-element method, which was the method that all teams used in carrying out their predictions. The students were advised by three faculty members who were experienced in the area of computational fracture mechanics. However, neither the students nor the faculty advisors had previously participated in an SFC.

The objectives of the final class project, as articulated to the students, were to:

- Learn about and become immersed in one of three finite-element-based methods for predicting fracture: adaptive remeshing (Ingraffea 2007; Spear et al. 2011; Wawrzynek et al. 2009), element deletion (Song et al. 2008; Lee et al. 2009), or the eXtended Finite Element Method (Mohammadi 2008; Pommier 2011);
- Conduct outside-of-class research related to the assigned fracture-simulation method;

- Think creatively about how to apply concepts from lectures to the project;
- Compare and contrast fracture predictions among the different computational methods.

From the perspective of the faculty advisors, the objective was to organize the execution of the project such that student participation was tractable within the constraints of the course and the students' knowledge and experience.

In the following section, an overview of the challenge scenario for SFC3 is presented. Section 3 focuses on the University of Utah teams' predictions, beginning with a description of how the project was organized and managed throughout the semester-long course. Section 3.1 includes a description of the general technical approach that the students pursued. Specific details of each simulation method, including approaches for calibrating damage and fracture parameters, are provided in Sect. 3.2. Section 4 presents prediction results of each team. Finally, Sect. 5 offers an in-depth discussion of both technical and organizational aspects of the project, and recommendations are provided for future classroom participation in SFC or similar round-robin activities.

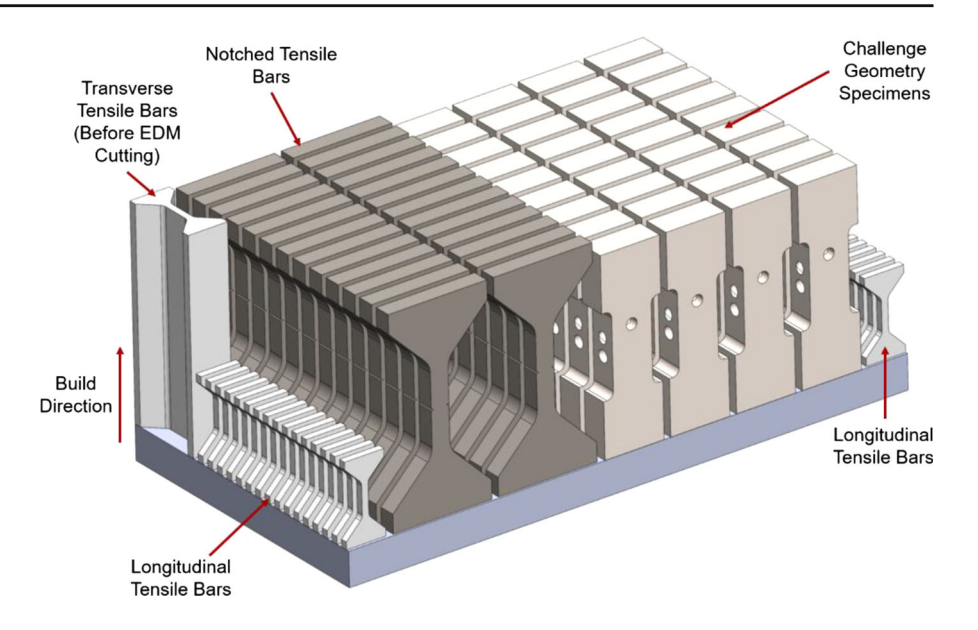
# 2 Overview of the third Sandia Fracture Challenge

The intent of the SFC3 was to assess, through a blind-prediction approach, the ability of the computational-fracture-mechanics community to predict ductile fracture in a challenge geometry produced via additive manufacturing (Kramer et al. 2019). The geometry was designed such that it would be nearly impossible to manufacture using conventional, subtractive processes and such that no closed-form solutions exist for prediction of failure. The challenge geometry included a hole, an internal cavity, and multiple internal channels. In total, 36 challenge specimens were manufactured using laser powder bed fusion of 316L stainless steel powder.

In addition to the challenge specimens used to assess blind predictions, two different types of calibration specimens (see Fig. 1) were manufactured and tested to provide participants with data to calibrate their models. The calibration specimens included both un-notched and notched samples tested in tension. The un-notched samples were fabricated in both longitudinal and transverse directions, while the double-notched samples were fabricated only in the longitu-



Fig. 1 Build design for the challenge and calibration specimens that were manufactured and tested as part of the SFC3.
Calibration specimens included un-notched and double-notched tensile bars. Specimens were manufactured using laser powder bed fusion of 316L stainless steel powder.
Reprinted with permission from Kramer et al. (2019)



dinal direction corresponding to the build direction of the plate. The challenge-geometry specimens were fabricated and tested in the build direction of the plate. Challenge-geometry and calibration specimens were all manufactured in the same build, as shown in Fig. 1. Details regarding specific data that were provided to participants are described in Sect. 2.1.

The SFC3 was designed to highlight the role of both intrinsic and extrinsic factors, such as material and dimensional variations, on estimating the behavior of additively manufactured samples. In addition to predicting global measures of load and displacement, participants in SFC3 were asked to predict local measures of strain, as described in Sect. 2.2. The participants could optionally provide 20%-lower and 80%-upper bounds on their predictions.

In the past, the SFC relied on predictions from volunteer experts in the field of computational mechanics to highlight the state-of-the-art and to uncover any limitations of the current computational approaches. However, for the first time, the SFC3 served as a platform for graduate students to put their knowledge of fracture mechanics into practice in a classroom setting.

### 2.1 Data provided

An extensive amount of data was provided by Sandia National Laboratories to all participants, and the reader is referred to Kramer et al. (2019) for a complete description of the provided data. In this work,

the faculty advisors elected to provide students with a subset of data to ensure that the focus would remain on the objectives of the course and that students could tractably make predictions within the scheduling constraints of the course. For example, the Utah teams did not use data pertaining to porosity, microstructure, and surface roughness (from X-ray computed tomography scans), since investigating the roles of these features was beyond the scope of the course objectives. Here, only the provided data or information that were used by the University of Utah teams are described.

All SFC3 participants were provided with technical drawings for the calibration and challenge-geometry specimens, which can be found in the lead article by Kramer et al. (2019). Additionally, force-versusdisplacement data were provided for the un-notched and double-notched samples, which was used to calibrate material and damage/fracture models, respectively. The Utah teams investigated both longitudinal and transverse data for the linear-elastic material properties and concluded that anisotropy would be negligible in the elastic region. They did not, however, consider the transverse data for the plastic region, even though anisotropy might have been critical in modeling plastic flow. Thus, the Utah teams used the longitudinal data from un-notched tensile tests to calibrate their elastic-plastic constitutive models and the longitudinal data from the double-notched tensile tests to calibrate models for evolution of damage and fracture, which will be discussed in detail in Sects. 3.2 and 3.3.



### 2.2 Quantities of interest

All participants in the SFC3 were asked to report a variety of quantities of interest (both local and global) based on the challenge specimen to facilitate comparison of the numerical analysis with the experimental results. The local quantities of interest were unique to this particular SFC. In SFC3, participants were asked to report six distinct quantities of interest based on their blind predictions of the challenge specimen: (1) force at defined displacements (0.25, 0.50, 0.75 and 1.0 mm); (2) force and Hencky (logarithmic) strain in the vertical direction at defined point locations on the specimen surface at four specific loads relative to peak load; (3) force versus gage displacement; (4) force versus Hencky strain in the vertical direction at defined point locations on the specimen surface; (5) force and Hencky strain in the vertical direction along four horizontal lines on the specimen surface at four specific load levels relative to peak load; and (6) images of the Hencky strain field on the specimen surface at crack initiation and complete failure. Figure 2 shows the locations at which the quantities of interest were to be reported. The reader is encouraged to see the lead article by Kramer et al. (2019) for a complete description of questions and associated points/locations. All participants were also asked

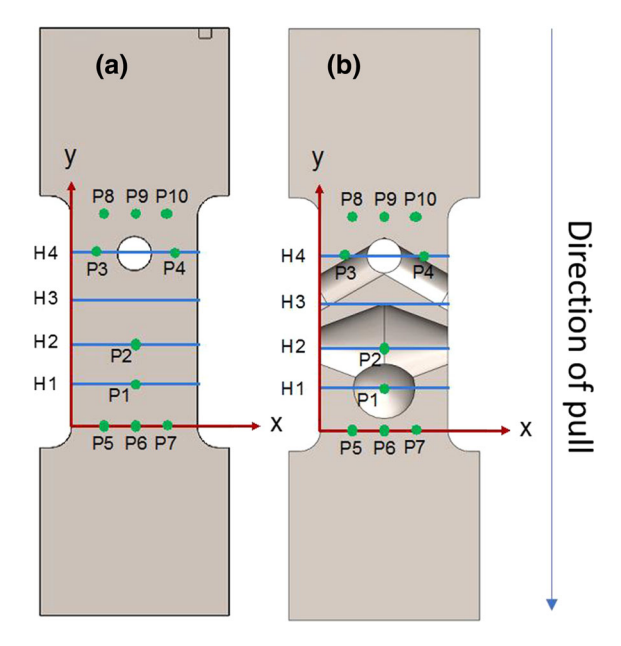
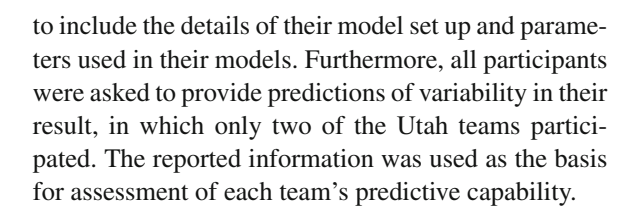


**Fig. 2** Annotated surface of challenge geometry showing the reference locations used for reporting the quantities of interest in the SFC3. Reprinted with permission from Kramer et al. (2019)



### 3 Methods

# 3.1 Project organization and management

The timeline for the class project was organized within the schedule of the semester-long course, as follows. The entire course spanned 16 weeks and was divided into the following topic areas, or modules: linear elastic fracture mechanics (LEFM), generalized (nonlinear) fracture mechanics, fatigue, and special topics. The lecture-by-lecture schedule included in the course syllabus is provided in the "Appendix" for reference. The project was first introduced to the students at the end of the sixth week of class (February 15, 2017), after the students had completed the module on LEFM. Although all SFC3 predictions were due to Sandia National Laboratories by mid-July of 2017, the students were required to complete their predictions and submit their final projects by the end of the semester on May 1, 2017. Thus, the students had approximately ten weeks to complete their predictions. Simultaneously, the students had to complete weekly homework assignments related to the above-mentioned topic areas.

The students were assigned to work in teams of two<sup>1</sup> and to apply one of three finite-element-based methods (mentioned in Sect. 1) to complete their predictions. The course instructor (Spear) was assisted by two other faculty members (Czabaj and Newell) to advise the teams. An undergraduate student (Ichi) was also recruited to compile and format the necessary files for submission after the semester had ended.

To accommodate the timeline described above and to place emphasis on the learning objectives for the project (namely, using fracture/damage models and calibrating their respective parameters), the faculty advisors performed some preliminary work that was considered to be outside the scope of the student-



One of the teams (Team E) had four members to share the load of modifying and running external scripts for material-state mapping.

Weeks 1-3	Weeks 4-7	Weeks 8-10
Learn/demonstrate method	Perform fracture/damage model calibration	Apply calibrated model parameters* to challenge specimen. Write report

<sup>\*</sup>some teams revisted their calibration during this time

Fig. 3 Graphical representation of timeline showing the number of weeks allocated for each of three deliverables associated with the SFC3 class project

learning objectives. Specifically, the advisors generated and shared CAD models of the double-notched specimen, grips, and challenge-geometry specimen; although, the latter was not disseminated to the students until after they had tackled the calibration procedure. Additionally, the advisors performed an initial calibration of material properties to capture the nominal elastic and plastic response of the un-notched tensile specimens (i.e. prior to incorporating any fracture or damage models). The students were encouraged to revisit the material-model calibration and tune it further once they incorporated their respective fracture or damage models. The students were also provided with Python scripts to extract, in a consistent manner, the load versus extensometer readings from an Abaqus® output database. Thus, the students' primary focus was on learning about, implementing, and calibrating their fracture or damage models and understanding how mesh sensitivity influences the predictions for a given method.

Rather than setting one final deadline and deliverables for the students, several deadlines and deliverables were defined throughout the semester to help maintain tractability and facilitate progress. The high-level tasks associated with each deliverable included: (1) learning about the assigned fracture-simulation method and demonstrating its application, (2) identifying and calibrating the relevant fracture or damage parameters based on experimental data from the double-notched specimens, and (3) applying the calibrated parameters to the challenge-geometry model to make blind predictions. Figure 3 provides a visual depiction of the amount of time the students spent on each of these tasks.

The first deliverable for the project was due three weeks after the project was introduced to the students. In this deliverable, students were required to familiarize themselves with the quantities of interest [described in Sect. 2.2 and in Kramer et al. (2019)], develop a plan for acquiring those quantities, perform at least one sim-

ulation of crack growth in the double-notched geometry with an arbitrary set of fracture/damage parameters, critically assess the differences observed between experimental and simulated load-versus-extensometer readings, and conjecture which model parameters should be adjusted to improve comparison with experiment. The students were not given formal instruction on their assigned simulation method and were instead prompted to perform outside-of-class research to learn about the method and how to apply it. Most of the students resorted to online tutorials, software documentation, and discussions with the faculty advisors to rapidly familiarize themselves with the modeling approaches. As mentioned previously, three of the students had no prior instruction in any finite element methods.

The second deliverable for the project was due four weeks after the first deliverable. During that four-week period, students focused on calibrating the damage or fracture parameters (and on fine tuning the initial material properties provided by the faculty advisors) using experimental data for the double-notched tensile specimens. Many of the teams accomplished this through a trial-and-error approach, by adjusting the parameters of their models until they were satisfied with the correspondence to the experimental load-versus-extensometer curve(s). Some of the teams took a more systematic approach by performing a sensitivity analysis to determine the influence that each parameter had on the results and using the information obtained to guide their parameter selection.

The final deliverable was due three weeks after the second deliverable. During that three-week period, students focused on applying their calibrated model parameters to the challenge-geometry model. The students were encouraged to perform a mesh sensitivity analysis and, in the process of doing so, some realized that they needed to revisit their calibration. For their final deliverable, students submitted reports that



followed a similar format as requested for the SFC3. They also prepared and delivered brief oral presentations describing their modeling process, calibration approach, simulations, and final results. Each team also answered questions raised by either faculty advisors or their fellow classmates. The presentations offered an opportunity for the teams to convene and debrief regarding the differences and similarities among modeling approaches.

### 3.2 General technical approach

The Utah teams (denoted here and in the lead SFC3 article (Kramer et al. 2019) as "Teams E-K") employed three different finite-element-based approaches to simulate fracture for the SFC3. All teams were required to use Abaqus® (Abaqus 2014) as the solver for several reasons: (1) the faculty advisors were experienced with Abaqus®, (2) the software was available to every student, and (3) Abaqus® offered several approaches for modeling ductile fracture. Three teams employed an adaptive-remeshing technique that required the use of a fracture-based remeshing software called FRANC3D (Wawrzynek et al. 2009) in conjunction with Abaqus® version 6.14 as the finiteelement solver. One of the adaptive-remeshing teams (Team E) employed an in-house, material-state mapping code to facilitate mapping of state variables from one mesh to the next following remeshing. The other two adaptive-remeshing teams (Teams E\* and E\*\*)<sup>2</sup> did not employ material-state mapping; however, they developed unique approaches to incorporate the effects of elasto-plastic crack propagation. The remaining teams employed damage or fracture simulation tools implemented within Abaqus®, in which cases the models were not remeshed during fracture simulation. Three of the teams (Teams F-H) used the element-deletion capability within Abaqus® version 6.14, and three teams (Teams I–K) used the Abaqus®

version 6.14 implementation of the eXtended Finite Element Method (XFEM).

Each Utah team modeled the material as isotropic, homogeneous, and rate-independent with an elasticplastic constitutive response (namely, J2 plasticity). All teams used a piecewise (tabulated) user-defined plasticity model in Abaqus to define the hardening behavior. As described in Sect. 3.1, the faculty advisors performed an initial material-model calibration (not accounting for fracture or damage evolution). In this initial calibration, the elastic modulus was determined based on the unloading portion of the stress-strain data from un-notched, longitudinal, tensile tests of AM 316L. The Poisson's ratio was taken to be 0.3, which is within the range of values reported for 316L stainless steel. The post-yield stress-strain response was approximated based on the provided experimental data from the un-notched, longitudinal samples. To account for significant necking in the samples between the point of peak stress and final rupture, the tabulated stress values were adjusted until the force-elongation response of the finite-element model matched the experimental data. This "true-stress" versus strain response was provided to the student teams as a starting point for their project. However, the teams were not required to use the provided model, and some teams elected to calibrate their own model instead.

Following an initial material-model calibration, each team then set out to calibrate the fracture/damage parameters associated with their respective simulation method. All teams used the same idealized geometry of the double-notched sample based on the technical drawings provided by Sandia National Laboratories. A slight notch radius was defined in the geometry based on representative notch radii shown in the optical micrographs provided by Sandia for the doublenotched samples. During the process of calibrating the fracture/damage parameters, the teams made further adjustments to their initial material models with the objective of capturing the first part of the load-versusextensometer curve, i.e. up to the point of peak-applied load, for representative double-notched tensile sample(s). The teams assumed that any subsequent drop in load (resulting in a deviation between simulation and experiment) was associated with either crack initiation or an increment of crack extension, which is consistent with basic theory of fracture mechanics. "Initiation" is used here to mean the first instance or appearance of a discontinuity in the model, and



<sup>&</sup>lt;sup>2</sup> The predictions from Teams E\* and E\*\* were not submitted to the SFC3 because the teams neglected to write out logarithmic strain, which was a required quantity of interest for participation (see Sect. 2.2). Consequently, any results involving logarithmic strain described in this manuscript do not include predictions from Teams E\* and E\*\*. The team names are assigned "E\*" and "E\*\*" to associate them with "Team E", originally named in the lead SFC3 article (Kramer et al. 2019), since all three teams used the adaptive-remeshing technique.

 Table 1
 Summary of elastic constants used in the final challenge model

	Young's modulus [E (GPa)]	Poisson's ratio (v)
Team E (adaptive remeshing)	93.9 <sup>a</sup>	0.3
Team E* (adaptive remeshing)	407 <sup>b</sup>	0.3
Team E** (adaptive remeshing)	183	0.3
Team F (element deletion)	173	0.3
Team G (element deletion)	194	0.3
Team H (element deletion)	160	0.3
Team I (XFEM)	173	0.3
Team J (XFEM)	173	0.3
Team K (XFEM)	200	0.3

<sup>&</sup>lt;sup>a</sup>Team E used the initial part of the stress-strain curve (instead of the reloading portion) to estimate the modulus

"extension" is used to mean any subsequent propagation of an existing discontinuity. The objective of the fracture/damage parameter calibration was then to try and match the remaining portion of the load-versusextensometer curve following peak load for a representative double-notched sample(s). Table 1 provides the modeled elastic properties, and Fig. 4 shows the plasticity and hardening responses used by each team for the final challenge model. Details regarding the methodspecific calibration procedures and the final calibrated fracture/damage parameters are provided in the next section.

All teams used the same, idealized geometry for the challenge model. The geometry was modeled based on the technical drawings provided by Sandia National Laboratories. No flaws, including surface roughness or porosity, were included in the challenge-geometry model. Teams G and J used quarter symmetry to decrease the computational cost. They ensured that their results were not impacted by additional constraints due to the symmetry boundary conditions by running a preliminary full-sized, uncracked model for comparison. All other teams used the complete geometry.

All teams applied approximately the same boundary conditions. Specifically, the teams attempted to replicate the applied boundary conditions from experiment by constraining their models in the regions of contact

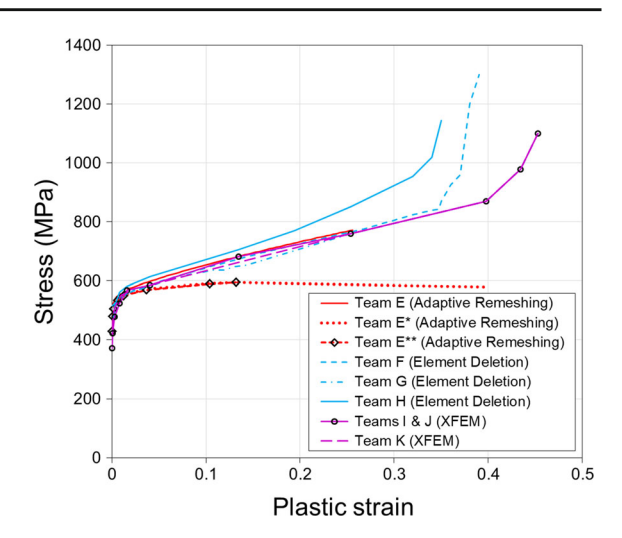
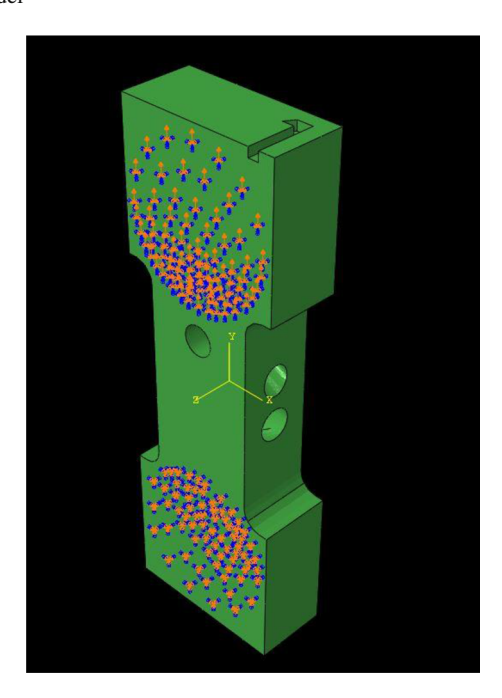


Fig. 4 Approximation of true stress versus plastic strain curves used in Abaqus<sup>®</sup> metal plasticity models for the final challenge model



**Fig. 5** A representative depiction of boundary conditions applied to the challenge-geometry model. Node sets corresponding to the regions of contact with the carbide pads from the grips had boundary conditions applied to represent realistic conditions from experiment. Here, all highlighted nodes were fixed in the x and z directions. Highlighted nodes on one of the grip ends were additionally fixed from displacement in the y direction, while non-zero displacement was applied in the y direction to highlighted nodes on the opposite grip end

between the specimen and the carbide pads of the grips, as shown in Fig. 5.



<sup>&</sup>lt;sup>b</sup>Team E\* calibrated Young's modulus by fitting the elastic portion of the force-displacement curve of a representative double-notched sample

# 3.3 Method-specific technical approaches

# 3.3.1 Adaptive remeshing (with and without material-state mapping)

Generally, in the adaptive-remeshing approach (Ingraffea 2007), crack initiation involves the explicit insertion of a crack(s) in a location(s) specified by the user. Following crack insertion, crack propagation is predicted point-wise along a three-dimensional crack front based on a user-specified growth criterion, and the geometry and mesh of the model are updated accordingly for each new increment of crack growth. The adaptive-remeshing technique used by Teams E, E\*, and E\*\* required the teams to define the conditions for crack initiation (i.e. at what numerical time step and spatial location to manually insert cracks into the model) and crack propagation (i.e. at what numerical time step to propagate the crack(s) and in what direction the crack(s) should kink). All three teams used Abagus/Standard® as the finite-solver and the software FRANC3D (Wawrzynek et al. 2009) to facilitate remeshing following incremental crack growth. FRANC3D currently supports prediction of linearelastic crack growth, such that any evolved variables, including displacements and plastic strains, are reset to zero following incremental crack growth and remeshing. This results in a sequence of simulations corresponding to different crack lengths with initially undeformed and unstressed states. Thus, to incorporate the effects of plasticity during crack extension, all three teams implemented creative solutions in their predictions, described below.

Team E used in-house codes (Spear et al. 2011) to facilitate material-state mapping following adaptive remeshing and to predict crack propagation based on a nonlinear fracture parameter. To define the conditions required for crack initiation, Team E first simulated a representative double-notched sample without any cracks. Crack initiation was assumed to occur at the numerical time step when the simulated load began to exceed the experimental load at a given increment of applied displacement. At that time step, the team calculated the volume-averaged value of maximum-principal strain within a cylindrical volume (0.1 mm radius) surrounding each notch. A radius of 0.1 mm was chosen to match the length of the initial crack to be inserted, which was 0.1 mm for both the notched specimen and challenge geometry. The calculated value of volume-averaged maximum principal strain (0.087) then served as the crack-initiation criterion for the challenge-geometry simulation. In the challenge model, a volume of the same radius was evaluated at each potential initiation site, and cracks of radius 0.1 mm were inserted (initiated) at locations meeting the same conditions as determined from the double-notched simulation. Crack propagation was determined based on critical crack-tip displacement (CTD), accounting for all three modes of displacement (Sutton et al. 2007; Lan et al. 2007; Spear et al. 2011):

$$CTD = \sqrt{CTD_I^2 + CTD_{II}^2 + CTD_{III}^2}$$

A calibration procedure similar to that used for initiation was implemented by Team E to determine the critical CTD required for crack propagation, such that the load-versus-extensometer curve for the representative double-notched sample could be reproduced. The critical value of CTD was found to be 0.02 mm evaluated at a distance of 0.01 mm behind each crack-front node. Since the model was remeshed after each increment of crack growth, in-house codes were used to map the displacements to the new mesh from the numerical time step at which propagation was predicted. Subsequently, the mesh-to-mesh solution mapping function in Abaqus® (version 6.14) was invoked to map remaining state variables onto the deformed mesh. The reader is referred to Spear et al. (2011) for specific details regarding the codes and procedures used to map material-state variables following crack propagation and remeshing by FRANC3D.

Because Teams E\* and E\*\* did not employ materialstate mapping, the material state was reset to zero following each increment of crack propagation and remeshing. To account for the plasticity that would otherwise accrue with crack extension, the teams sought to calibrate apparent R-curves by applying a postprocessing step that is best illustrated by Fig. 6. First, the teams simulated an uncracked double-notched specimen and identified the point at which crack initiation was assumed to occur (i.e., where the experimental and simulated force-displacement curves diverged). The teams then traced an elastic-unloading curve from the point of crack initiation, as shown in the Fig. 6, to identify a displacement value that would represent the effect of any residual strain in the model. Following crack insertion, remeshing, and simulation from a zerostate, both teams applied an offset to the simulated displacement curve by an amount equal to the aforemen-



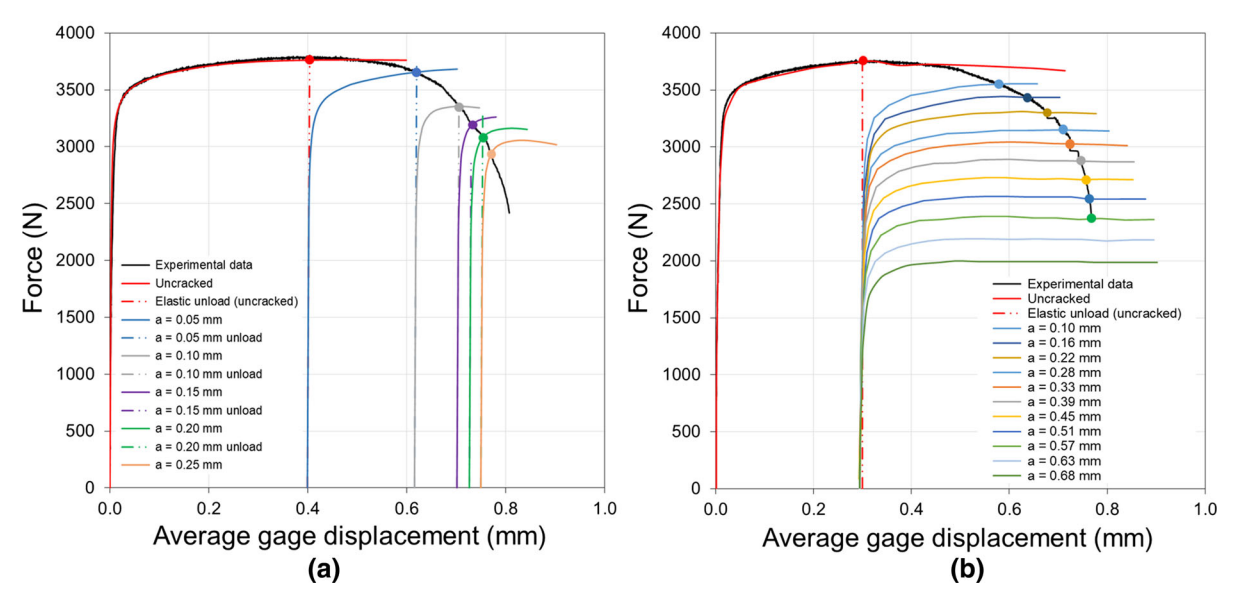


**Fig. 6** Method used for calibrating R-curve when using adaptive remeshing without material-state mapping: **a** Team E\*, **b** Team E\*\*. Points of intersection between each crack-length-dependent

reloading curve and the experimental force-displacement curve mark the crack-extension condition  $K_I(a) = K_{Ic}(a)$ 

tioned displacement value. Subsequently, the objective was to find the amount of displacement needed such that the offset force-displacement curve from simulation intersected the experimental curve, thereby indicating a critical state for crack extension. In the case of Team E\*, the process was repeated by tracing the elastic-unloading curve from each point of crack extension to the displacement axis and offsetting the next simulation response by that displacement amount, as indicated in Fig. 6a. For Team E\*\*, however, the simulated response corresponding to each new increment of crack extension was offset only by the original amount of displacement corresponding to crack initiation, as indicated in Fig. 6b. After performing a sufficient number of crack-growth simulations to capture the majority of the experimental force-displacement curve, both teams then used FRANC3D to calculate the mode I stress intensity factor,  $K_I$ , at the numerical time step where each intersection point occurred. These values of  $K_I$  were considered to be the apparent fracture toughness,  $K_{Ic}$ , corresponding to different crack lengths. The teams then plotted the  $K_{Ic}$  versus crack extension, da, to derive an apparent R-curve that could be used to predict crack extension in the chal-

lenge model. The resulting R-curves for both teams are shown in Fig. 7. Note in Fig. 7a that Team E\* calibrated a decreasing R-curve, which is physically unrealistic. From an energy-balance perspective, Team E\* effectively "redistributed" the energy dissipation that was likely associated with plastic deformation in the real specimen to energy dissipation by fracture, which resulted in a decreasing fracture toughness with increasing crack extension. The implications of this approach are discussed further in Sect. 4.1.

For all three adaptive-remeshing teams, quadratic tetrahedral elements (C3D10) were used for the majority of the challenge-geometry model. Along the crack front, a template of wedge, hexahedral, and pyramid elements were used, as described by Wawrzynek et al. (2009). In the regions nearest the crack front, the teams used element sizes on the order of 0.01 mm, and the meshes was coarsened dramatically with distance from the crack surface. The total number of elements in the challenge-geometry models increased with simulated crack advancement, which is characteristic of the adaptive-remeshing technique.

Teams E, E\*, and E\*\* used the information gleaned from their respective calibration procedures to predict crack initiation and growth in the challenge-geometry model. All three teams inserted cracks in locations of



 $<sup>\</sup>overline{^3}$  Despite violation of the small-scale yielding assumption,  $K_I$  is used as a surrogate to represent the relevant crack-front fields.

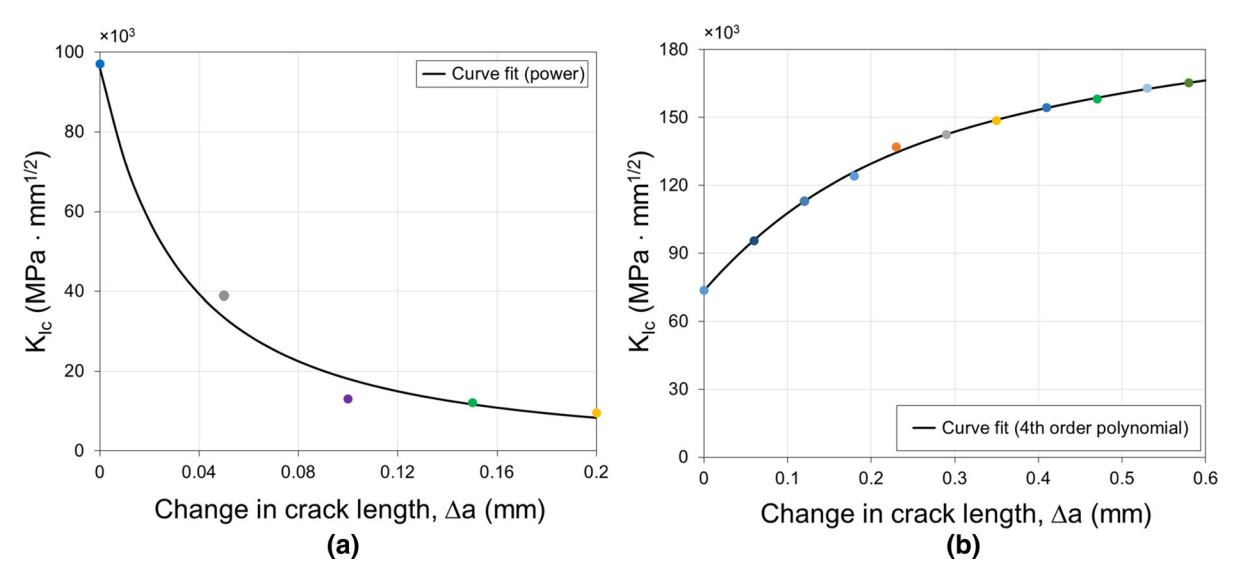
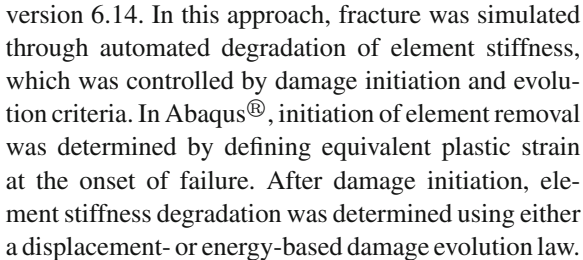


Fig. 7 Calibrated R-curves from carrying out the method shown in Fig. 6: a Team E\*, b Team E\*\*. The points are colored to correspond with the intersection points shown in Fig. 6a, b, respectively

maximum principal strain, and all three teams used the maximum tangential stress criterion (Erdogan and Sih 1963) implemented within FRANC3D to predict the local kink angle point-wise along the three-dimensional crack fronts. Team E propagated the cracks when the average CTD, evaluated 0.01 mm behind each crackfront node, reached the critical value of 0.02 mm. Teams E\* and E\*\* used their calibrated R-curves to predict when crack extension should occur for a given crack length (i.e., when  $K_I(a) = K_{Ic}(a)$  by evaluation of their respective R-curves). In generating their final load-versus-extensometer curves for the challenge-geometry model, Teams E\* and E\*\* applied their displacement-offset method by identifying the applied displacement at which  $K_I(a) = K_{Ic}(a)$  for a given crack length, extending the crack and remeshing, offsetting the subsequent reloading curve as described above, re-evaluating the R-curve to identify again when  $K_I(a) = K_{Ic}(a)$ , and repeating. Since multiple reloading curves were generated, the critical points from all curves were connected to form the final, predicted, force-displacement curve. The end result was a single curve that represented the entire load-versusextensometer response of the challenge model.

### 3.3.2 Element deletion

Teams F–H simulated fracture for the SFC3 using element deletion, implemented within Abaqus/Explicit®



Two element-deletion teams (Teams G and H) used critical fracture energy to initiate onset of element degradation, while one team (Team F) used critical displacement. Teams F and H used quadratic tetrahedral elements (C3D10 and C3D10M, respectively) and Team G used linear tetrahedral elements (C3D4) to mesh the challenge geometry. Because of the interdependency between mesh size and element-deletion parameters, calibration of damage parameters had to be performed in conjunction with a mesh-convergence study, carried out as follows. Prior to calibration, all teams performed a mesh convergence study on the double-notched specimen models to ensure satisfactory specimen response and "smooth" shape of the simulated fracture surfaces. An initial calibration of the element-deletion parameters was then performed with the converged mesh by modifying the parameters until the simulated load-extensometer response of the double-notched model matched that from experiment. After this initial calibration, the converged-mesh



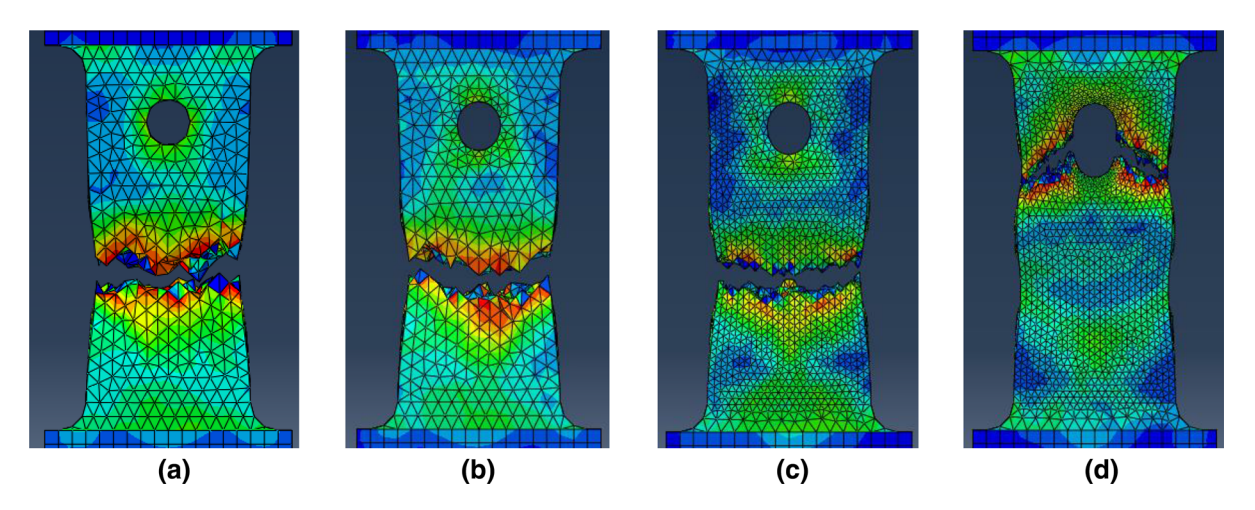


Fig. 8 Effect of mesh size on location and roughness of predicted failure surface using element deletion. Meshes have the following number of elements: a 22,553; b 29,548; c 107,186; d 147,558; e 838,178

Table 2 Summary of parameters used by the element-deletion teams

	Damage initiation			Damage evolution			
	Fracture strain	Stress triaxiality	Strain rate (s <sup>-1</sup> )	Туре	Displacement at failure (mm)	Fracture energy (J/m <sup>2</sup> )	
Team F (nominal)	0.430-0.480	0.0-1.0	0.00127	Displacement	0.0175	_	
Team F (lower)	0.300-0.350	0.0-1.0	0.00127	Displacement	0.03	_	
Team F (upper)	0.435-0.485	0.0-1.0	0.00127	Displacement	0.02	_	
Team G (nominal)	0.311	0.33	0	Energy	_	3673	
Team H (nominal)	0.48	0.33	0	Energy	_	3100	
Team H (lower)	0.46	0.33	0	Energy	_	3100	
Team H (upper)	0.52	0.33	0	Energy	_	3100	

Multiple entries indicate that multiple simulations were conducted to provide upper- and lower-bound predictions

size and element-deletion parameters were applied to the challenge-geometry model. Due to the complex shape of the challenge geometry, the teams used elements that were, on average, smaller than those used in the double-notched specimen model. The smaller element sizes were determined by performing a meshconvergence study on the challenge-geometry model to ensure that the locations of damage/fracture initiation were converged. Interestingly, all three teams found that by using the initial element size deemed converged for the double-notched model, failure initiated near the central, internal, elliptical void, regardless of elementdeletion parameters used. As the mesh was refined, the failure-initiation location transitioned upward towards the void with the smaller, circular cross section. This dependence of failure path on mesh size is shown in Fig. 8. In light of this discovery, all three teams performed a second round of parameter calibration on the double-notched model using a smaller mesh size. The calibrated parameters used in the challenge-geometry model are summarized in Table 2 for Teams F–H.

In addition to the nominal fracture predictions for the challenge-geometry model, Teams F and H made additional upper- and lower-bound predictions by calibrating two additional sets of damage parameters. To do so, both teams selected two experimental curves from the double-notch data that represented upper- and lower-bound responses. They then re-calibrated their damage parameters (i.e., fracture strain and, in the case of Team F, displacement at failure) to match the experimental bounds. Each team applied the parameters from the nominal, upper-, and lower-bound calibrations in three separate predictions of the challenge geometry.



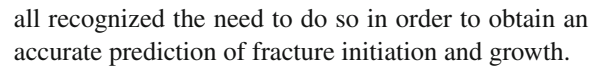
**Table 3** Summary of parameters used by the XFEM teams

	Damage initiation			Damage evolution		
	Max principal stress (MPa)	Max principal strain	Tolerance	Туре	Displacement at failure (mm)	
Team I	1200	_	0.1	Displacement	0.08	
Team J	_	0.35	0.05	Energy	0.08	
Team K	1200	_	0.1	Displacement	0.10	

# 3.3.3 Extended finite element method (XFEM)

Teams I–K adopted an XFEM approach to predict the fracture behavior in the SFC3. In this approach, elements must be enriched *a priori* with a step function that enables the representation of a discontinuity (Moës et al. 1999; Sukumar et al. 2000; Ingraffea 2007). The onset and/or growth of the discontinuity is determined from either a displacement- or energy-based fracture criterion. The increment of crack evolution is dictated by the size of the enriched elements, and crack initiation and growth can only occur in regions with enriched elements. In that regard, the XFEM approach for crack growth can exhibit mesh sensitivities.

Teams I-K used the implementation of XFEM within Abaqus/Standard® (version 6.14), which supports prediction of both fracture initiation and propagation. The model geometry was discretized using linear hexahedral elements with reduced-order integration (C3D8R) in the enriched regions where cracks were expected to initiate and propagate. For the rest of the domain (i.e., where cracks were not expected to initiate or propagate), Teams I and J used linear tetrahedral (C3D4) elements. Team K used quadratic tetrahedral (C3D10) elements away from where fracture was expected, which resulted in disconnected midside nodes on the boundary between different element types. However, this transition region was sufficiently far away from where fracture was expected to occur that Team K deemed this mismatch acceptable. Performing a mesh convergence study for the XFEM teams proved to be difficult due to the strong interdependence among damage parameters, mesh size/configuration, and plasticity. This interdependency led to difficulties in achieving converged numerical solutions for much of the time spent working on the project. Thus, it was intractable for the XFEM teams to perform a mesh convergence study in their abbreviated timeline for the SFC3, but



Two of the XFEM teams (Teams I and K) used maximum principal stress (MaxPS) as their fracture/failure criteria, and one (Team J) used maximum principal strain (MaxPE). The teams defined a damage tolerance of either 5% or 10%, allowing cracks to initiate within the range of 5% or 10%, respectively, of the specified fracture/failure threshold. The teams specified either displacement-based or energy-based damage evolution criterion with threshold values listed in Table 3. Similar to the other simulation approaches, the objective of the calibration procedure for the XFEM teams was to iteratively modify the damage initiation and evolution parameters until the simulated loadversus-extensometer response for an idealized doublenotched model matched the response from a representative experiment. The calibrated parameters used in the challenge-geometry model are summarized in Table 3 for Teams I-K.

### 4 Results and discussion

Figure 9 demonstrates the project evolution in terms of submitted deliverables for three representative teams, one from each type of simulation method. As described in Sect. 3.1, the first deliverable of the project was for the teams to learn about their respective method based on outside-of-class research and to demonstrate application of the method to the double-notch geometry. Force-versus-extensometer results from the first deliverable are shown in Fig. 9a, d, g for the three representative teams. As shown in the plots, the first attempt at applying each method did not yield satisfactory results when compared with experimental data. Thus, after learning how to apply their methods, each team spent a considerable amount of time examining the influence of the model parameters on the global forceversus-extensometer curves. Figure 9b, e, h show the



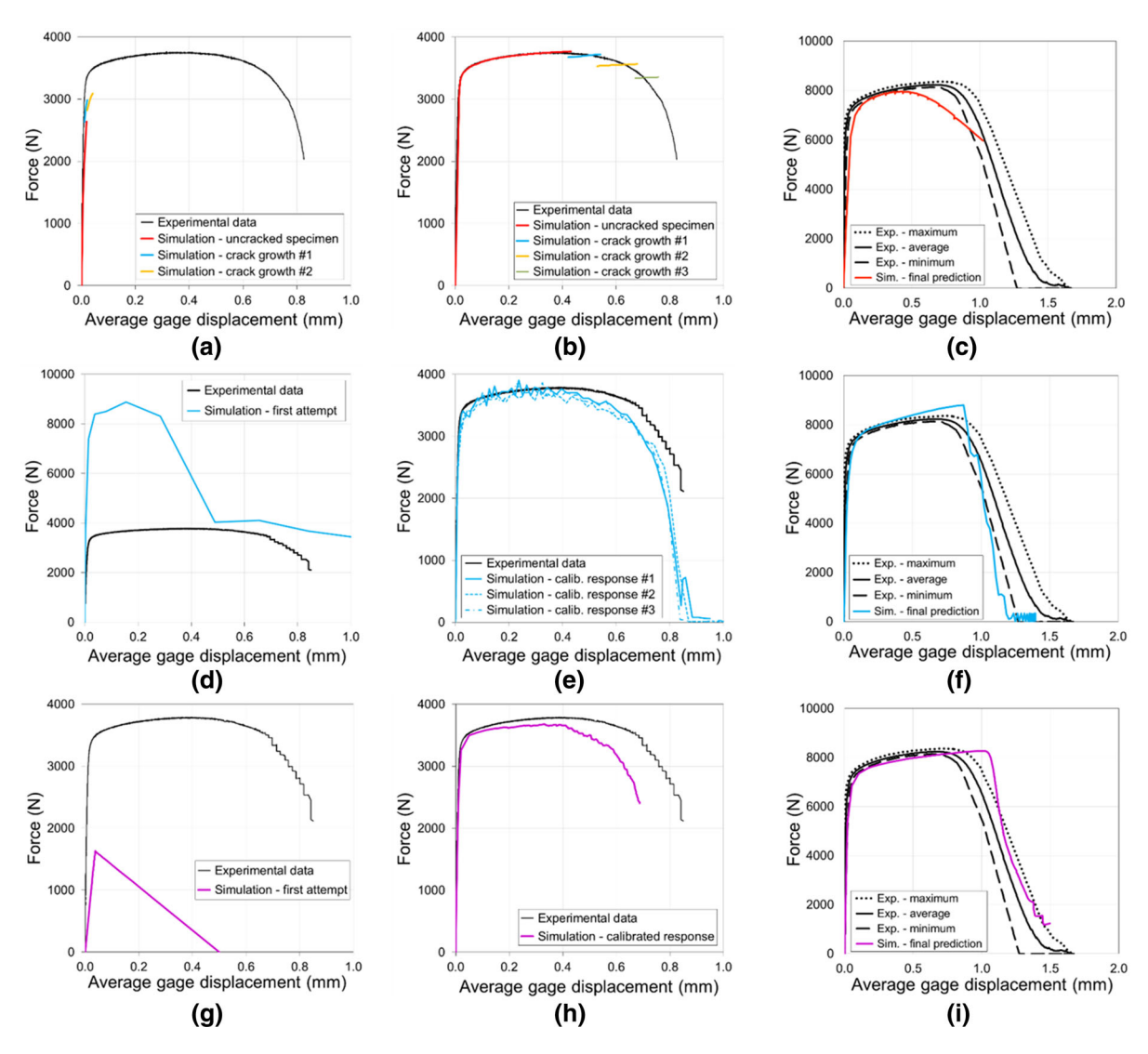


Fig. 9 Load-versus-extensometer results from a series of deliverables representing the evolution of the SFC3 class project for three representative teams:  $\mathbf{a}$ ,  $\mathbf{b}$ ,  $\mathbf{c}$  Team E (adaptive remeshing);  $\mathbf{d}$ ,  $\mathbf{e}$ ,  $\mathbf{f}$  Team H (element deletion);  $\mathbf{g}$ ,  $\mathbf{h}$ ,  $\mathbf{i}$  Team K (XFEM). Deliverable 1:  $\mathbf{a}$ ,  $\mathbf{d}$ ,  $\mathbf{g}$  first attempts at applying the respective

simulation methods; results are for the double-notch geometry. Deliverable 2:  $\mathbf{b}$ ,  $\mathbf{e}$ ,  $\mathbf{h}$  calibration results based on the double-notch geometry. Deliverable 3:  $\mathbf{c}$ ,  $\mathbf{f}$ ,  $\mathbf{i}$  blind predictions for the nominal response of the challenge geometry compared to experimental data provided after predictions were submitted

teams' submissions for the second deliverable, which was a calibration of their respective fracture or damage parameters using experimental data from the double-notch tests. It is noted that some of the teams revisited their calibration after submitting their second deliverable. For example, as mentioned in Sect. 3.3.2, some of the teams found that smaller element sizes were needed for convergence of the challenge-geometry model than what was needed for convergence of the double-

notch geometry. Consequently, the teams whose predictions exhibited mesh dependencies found that they needed to re-calibrate their damage/fracture models for the double-notch geometry after modifying the mesh refinement. Thus, the results from the second deliverable shown in Fig. 9b, e, h do not necessarily reflect the final parameters that were used for the blind predictions. The third deliverable for the project was to provide blind predictions for the challenge geometry.



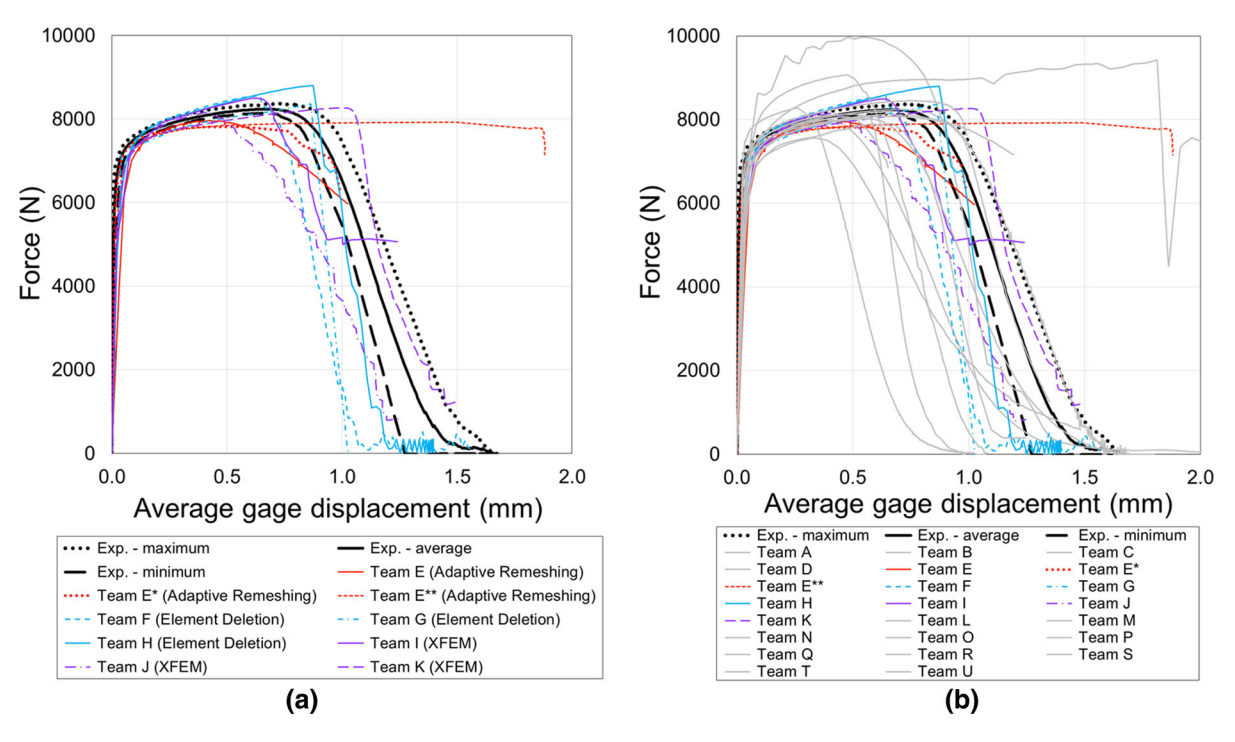


Fig. 10 Predictions of load versus gage displacement compared to experimental measurements for the challenge-geometry specimens from the SFC3. a Predictions from University of Utah teams only. b Predictions from all participating teams in

the SFC3. Predictions are color-coded based on the simulation approach used. Note that Teams E\* and E\*\* participated in the class project but did not submit predictions to the SFC3 and are therefore not counted among the official participant list

Figure 9c, f, i show the nominal predictions for each team compared to the experimental results, which were released after the blind predictions were submitted. Figure 9 clearly illustrates the progress made throughout the semester by participating in the SFC3.

# 4.1 Predictions and comparison of methods

The load-versus-extensometer predictions for the challenge geometry are plotted for all nine University of Utah teams, along with the experimental results, in Fig. 10a. Figure 10b additionally shows the predictions of all other teams who participated in the SFC3 (Kramer et al. 2019). As shown in Fig. 10, all Utah teams reasonably predicted the global response until an average gage displacement of about 0.5 mm, at which point discrepancies among the fracture methods and parameters begin to manifest. Given that the teams all followed approximately the same calibration procedure for the constitutive model (and, in fact, started with nominally identical material properties), it is not surprising that the predictions are quite similar until that

point. One important takeaway from this observation is that thorough calibration of the elastic-plastic constitutive model (prior to onset of fracture/damage) seemed to be as important as, if not more important than, the fracture model, given that the specimens experienced a significant amount of plastic deformation prior to onset of fracture.

The choice of fracture-simulation technique impacted the shape of the force-displacement curve for each team, as shown in Fig. 10. With the exception of Team J, predictions from element-deletion and XFEM teams all exhibit a fairly sharp transition in the force-displacement response, marked by an abrupt and sustained load drop. This is in contrast to the much smoother response of Teams E and E\*, both of which are adaptive-remeshing teams. Team E\*\* has the most divergent prediction among the University of Utah teams. This is related to the manner in which Team E\*\* calibrated and subsequently applied their R-curve. Recall, both Teams E\* and E\*\* developed methods to calibrate their R-curves by accounting for loss of prior plasticity following adaptive remeshing. As



shown in Fig. 6b and described in Sect. 3.3.1, Team E\*\* implemented an offset approach (to account for plasticity effects) in which the simulated load-displacement response for every crack-growth increment was shifted from zero to the displacement corresponding to elastic unloading at crack initiation. On the other hand, Team E\* applied progressively larger displacement offsets as the crack(s) propagated. Consequently, the resulting fracture toughness values (i.e., computed K<sub>I</sub> values when the offset load-displacement curves intersected the experimental curve) were larger and increasing for Team E\*\* and smaller and decreasing for Team E\*, shown in Fig. 7. By Team E\*\*'s approach, significantly more displacement is required to reach the condition for crack extension. This results in excessive ductility in the predicted global response, as shown in Fig. 10. Interestingly, Team E\* has a slightly better prediction of load versus displacement than even Team E, who incorporated material-state mapping. Note from Figs. 6a and 7a that Team E\*'s calibration method results in a decreasing R-curve, indicating that the resistance to fracture actually decreases with increasing crack growth. Physically, fracture toughness has been shown to increase with crack extension for some materials due to the increase in energy dissipation associated with inelastic processes (viz., plastic deformation) near the crack tip. For Team E\*, the reduction in plasticity-induced energy dissipation with increasing crack length is offset by reducing the fracture toughness, resulting in an artificial (yet calibrated) decreasing R-curve. While this result is likely non-physical, it appears that as long as the blind prediction is carried out in the same manner as that used to calibrate the Rcurve, the predicted response of the specimen actually matches experiment fairly well. This result suggests that it might be possible to simulate accurately the ductile tearing response using an adaptive-remeshing technique without the need to map material state variables. The validity of this statement hinges, of course, on the calibration procedure used, as highlighted above. This could potentially be a meaningful finding given the computational expense associated with material-state mapping, and the authors suggest that the approach implemented by Team E\* be explored further.

As shown in Fig. 10b, the University of Utah teams performed comparably to or better than many of the teams who participated in the SFC3. The exception to this is Team E\*\*, whose prediction was discussed above. According to the lead SFC3 article by

Kramer et al. (2019), two University of Utah teams ranked within the top five out of 21 participating teams based on an average-error ranking system of the force-displacement predictions; Teams H (element deletion) and K (XFEM) ranked 5th and 4th, respectively.

Figures 11 and 12 show the vertical logarithmic strain measured along horizontal lines H3 and H4 (defined in Fig. 2) at peak load from both experiment and simulation of the challenge-geometry specimens. With the exception of Team E (adaptive remeshing), the University of Utah teams all captured the local strain measurements in their predictions fairly well. Team F (element deletion) had the best strain predictions among the University of Utah teams. In fact, Team F was ranked 4th out of 21 participating teams based on an average R-squared error measure of strain-displacement response described in the lead SFC3 article (Kramer et al. 2019).

The discrepancy in Team E's prediction of logarithmic strain is related to the material-state mapping routine in Abaqus®, which the team leveraged in their simulations. Following crack extension and remeshing, Team E applied an in-house code to map the displacements from the previous mesh to the new mesh, thereby creating a deformed mesh with new surface area corresponding to crack extension. Once the deformed mesh was generated, the material-state mapping routine within Abaqus® (version 6.14) was invoked to transfer remaining state variables from the previous simulation to the new, deformed mesh. Interestingly, it was discovered through this SFC3 exercise that the solution-mapping algorithm in Abaqus® did not map logarithmic strains, which are a function of the deformation gradient. However, the stresses and plastic strains were mapped, as expected. Consequently, Team E's predictions of strains start out relatively close to the experimental values, but begin to underpredict dramatically at and after peak load, following crack growth and adaptive remeshing (Fig. 13).

In addition to reporting strain values along specific paths at specific load levels, all SFC3 participants were asked to provide figures of the full-field strain maps at crack initiation and final failure. Logarithmic strain maps predicted by the participating Utah teams are shown in Figs. 14, 15 and 16.

Some interesting comparisons can be made among the different simulation approaches by investigating Figs. 14, 15 and 16. Qualitatively, the shapes of the strain fields are similar across all Utah teams at



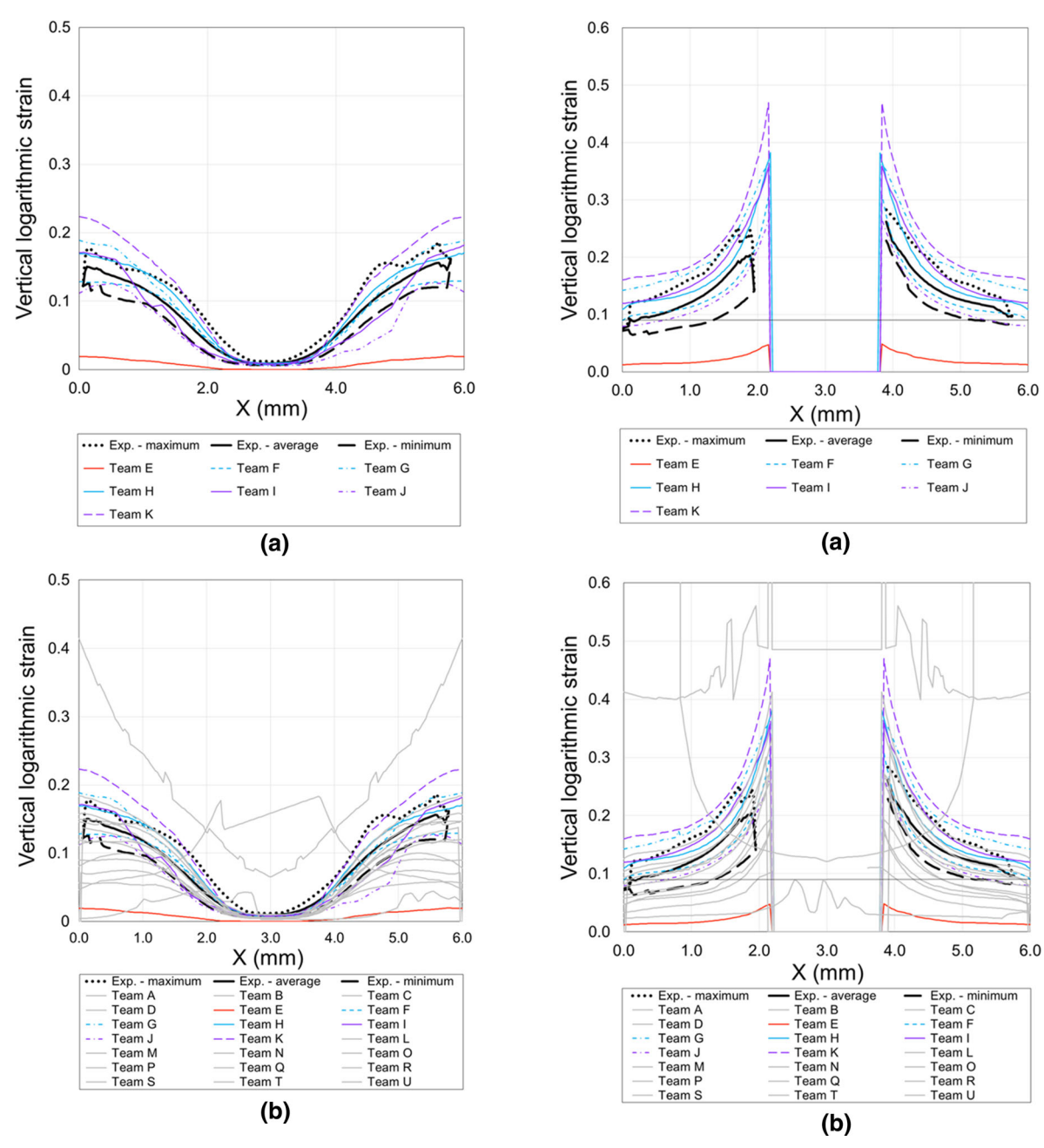


Fig. 11 Predictions of vertical logarithmic strain along the horizontal line H3 (see Fig. 2) at peak applied load compared to experimental measurements for the challenge-geometry specimens from the SFC3. a Predictions from University of Utah teams only. b Predictions from all participating teams in the SFC3 (Kramer et al. 2019). Predictions are color-coded based on the simulation approach used. Note that Teams E\* and E\*\* participated in the class project but did not submit predictions to the SFC3 and are therefore not counted among the official participant list

Fig. 12 Predictions of vertical logarithmic strain along the horizontal line H4 (see Fig. 2) at peak applied load compared to experimental measurements for the challenge-geometry specimens from the SFC3. a Predictions from University of Utah teams only. b Predictions from all participating teams in the SFC3 (Kramer et al. 2019). Predictions are color-coded based on the simulation approach used. Note that Teams E\* and E\*\* participated in the class project but did not submit predictions to the SFC3 and are therefore not counted among the official participant list



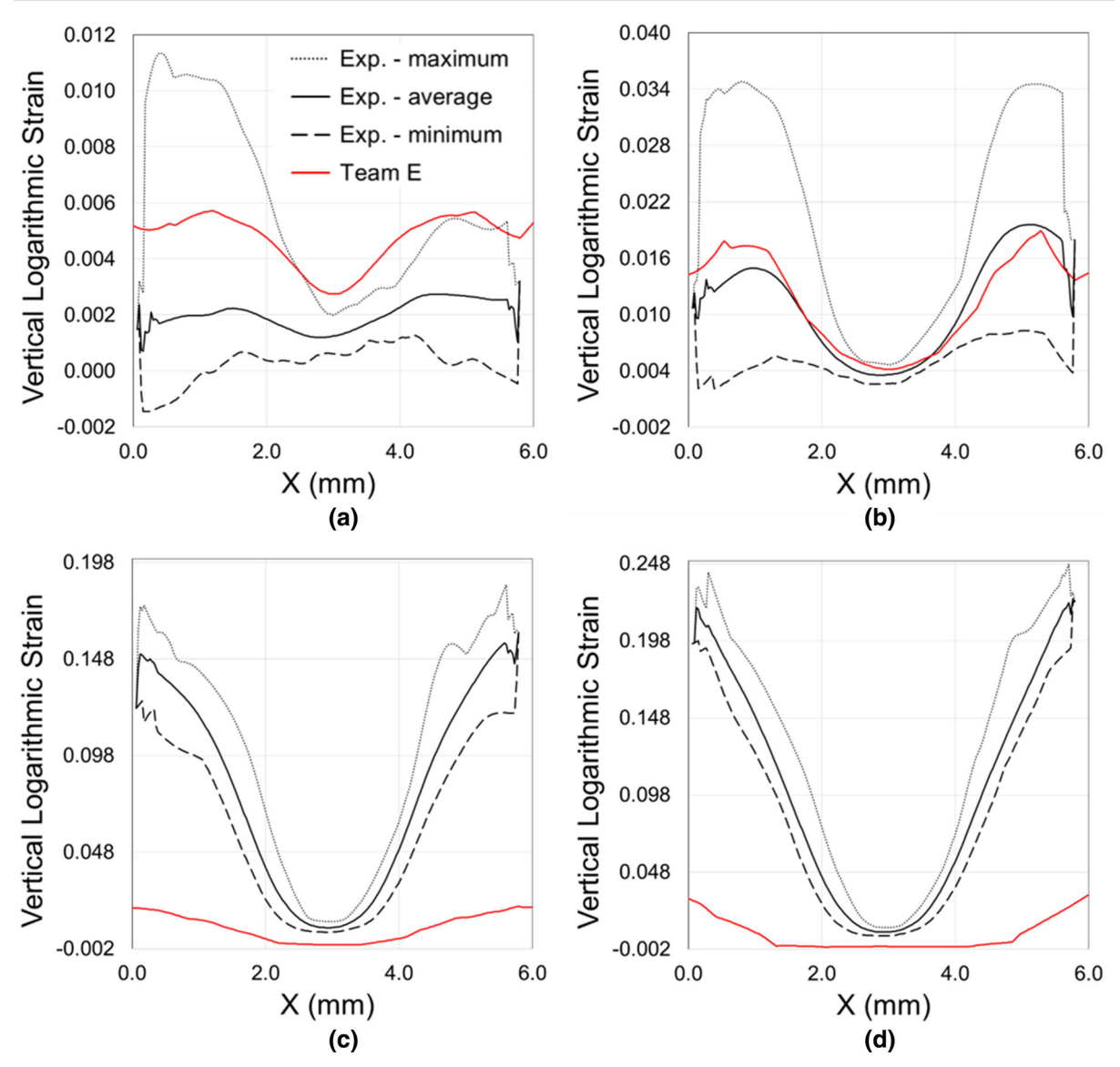


Fig. 13 Team E's predictions of vertical logarithmic strain along the horizontal line H3 (see Fig. 2) compared to experimental measurements at four load levels relative to peak load: a 75%, b 90%, c 100% (peak load), d 90% (after peak load)

crack initiation. However, there are differences in the predicted crack path and fracture-surface roughness among the various methods. First, note that the Utah teams all predicted crack initiation to occur near the four internal corners where the two angled channels intersect the through-thickness hole, regardless of the initiation criterion or simulation method employed. Following initiation, the adaptive-remeshing and XFEM teams predicted crack propagation along a nominal Mode I path, i.e. approximately normal to the applied-loading direction (see Fig. 16). This result was some-

what surprising given that the internal cavities and angled channels within the specimen were expected to cause a deflection in the crack path. The element-deletion teams, on the other hand, predicted the crack path to follow the path of the angled channel within the specimen. Teams F and H also predicted a slight deflection upward just prior to complete failure (see Fig. 15). Interestingly, both types of predicted crack paths (nominally Mode I and angled along the channel) were observed among the 36 specimens tested by Sandia for the SFC3 (Kramer et al. 2019).



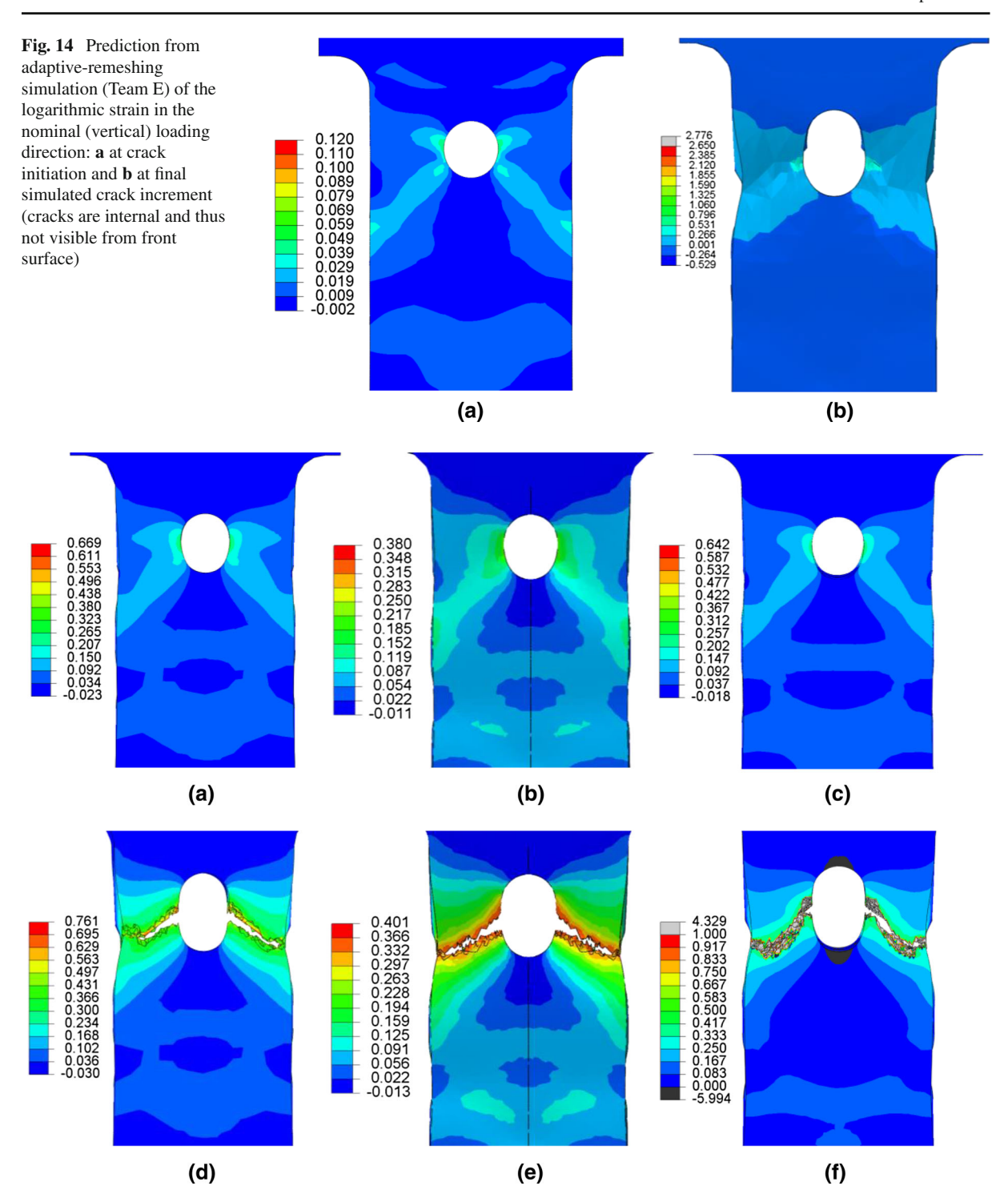


Fig. 15 Predictions from element-deletion simulations of the logarithmic strain in the nominal (vertical) loading direction at crack initiation (top row) and at complete failure (bottom row): a, d Team F; b, e Team H



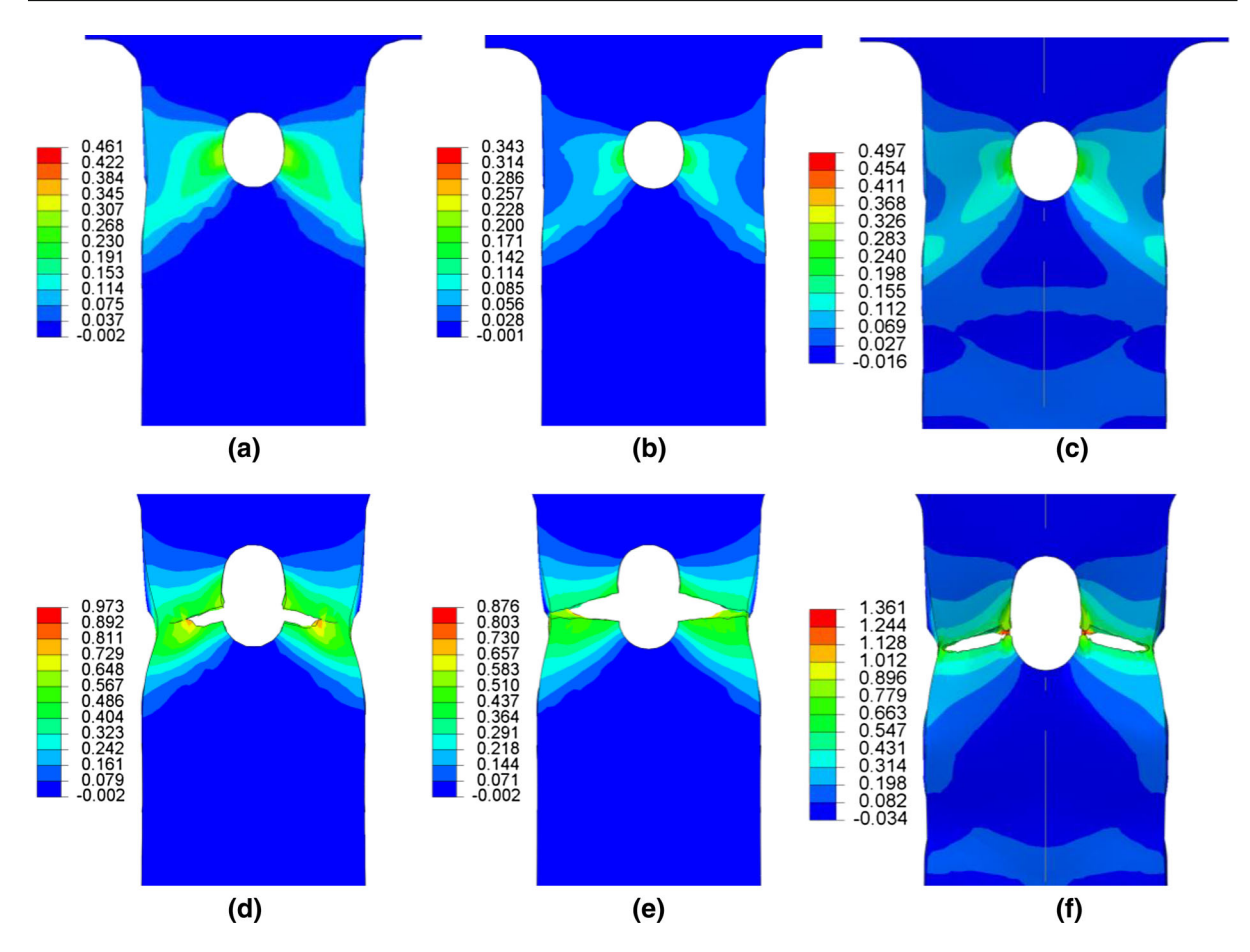


Fig. 16 Predictions from XFEM simulations of the logarithmic strain in the nominal (vertical) loading direction at crack initiation (top row) and at complete failure (bottom row): a, d Team I; b, e Team J; c, f Team K

In general, element-deletion simulations result in more tortuous crack-surface predictions than either XFEM or adaptive remeshing. In some cases, this tortuosity can appear to be quite realistic. However, this effect is a visual manifestation of removing elements from an unstructured mesh and is an artifact caused by the mesh dependency of the approach. As expected, the predicted fracture-surface roughness tends to decrease with additional mesh refinement in this approach, as depicted earlier in Fig. 8.

Based on the experience of participating in the SFC3, the University of Utah teams have identified advantages and disadvantages of all three simulation approaches. Among the three methods (adaptive remeshing, element deletion, and XFEM), adaptive remeshing exhibits the least mesh sensitivity, which is corroborated elsewhere in the literature (Ingraffea

2007). However, this approach is most computationally expensive, especially if material-state mapping is employed. In fact, the computational expense precluded the adaptive-remeshing teams from being able to simulate crack growth to complete separation of the challenge specimen (Fig. 14). Another important point regarding adaptive remeshing is that the technique is capable of predicting arbitrary crack propagation, but not crack initiation. Thus, the user must manually insert initial crack(s) using FRANC3D.

Similarly, the Abaqus<sup>®</sup> implementation of XFEM (version 6.14) offers both advantages and disadvantages. One disadvantage is that the method exhibits considerable mesh dependency. For example, the implementation within Abaqus<sup>®</sup> seemed to work well with hexahedral elements but not with tetrahedral elements, which presented modeling challenges since tetrahedral



elements were more amenable to meshing the complex challenge geometry. Additionally, the students found that the XFEM simulations were very sensitive not only to element type but also to element (mesh) size. In fact, some students found that the numerical solution would diverge if the mesh was too fine. The reason for these observed mesh dependencies remains unclear. In some cases, e.g. Fig. 16f, XFEM failed to completely separate elements even after meeting the failure criterion. Despite these mesh-related hurdles, the Abaqus<sup>®</sup> implementation of XFEM (version 6.14) was able to seamlessly handle plasticity with fracture and seemed to work well once an appropriate mesh was in place.

Perhaps the greatest advantage of element deletion was that it had a lower learning curve compared to the other methods, rendering it an attractive method for beginning practitioners. The method is relatively straight-forward to implement within Abaqus<sup>®</sup>, and as a result, the element-deletion teams were the only teams who were able to complete more than one simulation on the challenge geometry within the project timeframe. Consequently, this method seems to lend itself nicely to investigating sources of variability and performing parametric studies. The obvious disadvantage of element deletion, which was discussed earlier, is the pronounced mesh sensitivity. Additionally, it is important to note that element deletion does not technically simulate the evolution of a fracture surface. Nevertheless, it is shown to be a valuable tool for predicting ductile failure of metals.

### 4.2 Organization, management, and recommendations

In terms of organization and management of the SFC3 class project, the authors offer recommendations based on what worked and what could be improved for future participation in an SFC or similar round-robin activities. When the SFC3 was first issued by Sandia, a significant amount of data and information was provided by the organizers to all participants. The faculty advisors felt that simply releasing all this information and data to the students without carefully guiding their participation could lead to analysis paralysis. Thus, it is recommended that the faculty advisors take the following steps in a classroom setting to prevent such a scenario:

- Decide what aspects of participation are necessary
  or valuable for the course objectives, and actively
  assist students with other tasks that do not directly
  meet those objectives. For example, as described in
  Sect. 3.1, the faculty advisors generated CAD models and performed an initial material-model calibration for the students so that the students could
  spend their time on calibrating their damage or fracture models, which was consistent with the course
  objectives.
- Control the rate and influx of information. For example, the faculty advisors generated a CAD model of the challenge geometry early on in the semester, however, elected not to provide that to the students until they had finished calibrating their models against the double-notched specimen data. This allowed the students to maintain focus on one task at a time.
- Give students access to the information packet provided by the organizers, but discuss with students what information or data can be neglected in light of the course objectives. For example, the faculty advisors suggested that the students neglect (unless they chose otherwise) the X-ray tomography data and digital image correlation data provided in the original information packet (Kramer et al. 2019), as discussed in Sect. 2.1.
- Set clear and intermediate deliverables throughout the semester that allow the students to tackle individual tasks on their way to meeting the final goal. For example, the SFC3 project was broken down into three specific deliverables, as described in Sect. 3.1.

Given the scheduling constraints of the course and the limitations of both time and experience, the above recommendations are considered essential to maintain tractability of classroom participation on a project of this magnitude.

Additionally, the authors recommend that the following steps be taken, which were not taken in this work. First, the authors recommend that experience with finite-element analysis be a pre-requisite for participating in the project; experience with the intended software (Abaqus<sup>®</sup>, in this case) would be a plus. Recall that three of the 20 students had no such experience prior to taking the course. While those students were intentionally paired with someone who did have prior experience with finite-element analysis, it was



<sup>&</sup>lt;sup>4</sup> Analysis paralysis is a feeling of being overwhelmed (often caused by information overload) that leads to complete inaction.

often difficult for those teams to distribute the workload in ways that other teams could, which caused frustration for some of the students. Another recommendation would be to start the entire project earlier in the semester by having the students work through faculty-developed tutorials. While the initial intent of the instructor was to commence the project after the students had developed an understanding of LEFM theory, it seems, in retrospect, that this is not necessary. Furthermore, the students were instructed, in this work, to leverage existing tutorials and documentation to develop an understanding of the implementation of their respective methods. However, many of the students found the existing tutorials to be lacking for various reasons. Thus, the faculty advisors should develop specific tutorials that would provide more immediate guidance for the students early in the semester. Doing so would allow for more time to be spent troubleshooting and calibrating the damage or fracture models, as well as exploring the effects of material and geometrical variability on the predictions.

### 5 Conclusion

This manuscript describes the participation of an entire class of 20 graduate students at the University of Utah in the Third Sandia Fracture Challenge (SFC3). The purpose of the SFC3, which was issued in 2017 by Sandia National Laboratories, was to assess the ability of the computational-fracture-mechanics community to predict ductile fracture in a complex specimen geometry produced via additive manufacturing of stainless steel 316L powder (Kramer et al. 2019). Similar to previous SFCs, the SFC3 was conducted in a blind, round-robin style approach, where volunteer participants from around the world could submit predictions. In the SFC3, 21 teams participated, and seven of those teams comprised students from the graduate course at the University of Utah. When the SFC3 was first issued, participants were provided with a substantial amount of data, including mechanical-response data of un-notched and notched tensile specimens. The participants were then asked to make blind predictions of both global and local quantities of interest in the challenge geometry. Participants could optionally submit upper- and lower-bound predictions in addition to nominal predictions.

The University of Utah teams were advised by three faculty members, who helped to organize the project within the scheduling constraints of the course. The class was divided into teams and assigned one of three finite-element-based methods to apply to the SFC3: adaptive remeshing, element deletion, or the eXtended Finite Element Method (XFEM). Three primary deliverables were defined for the student teams: (1) learn about and demonstrate application of the assigned method, (2) calibrate the relevant fracture or damage parameters based on experimental data of double-notched specimens, (3) apply the calibrated parameters to the challenge-geometry model to make blind predictions of fracture.

In general, the University of Utah teams performed comparably to or better than many of the SFC3 participants. Out of the 21 teams who participated, three of the seven teams from Utah ranked among the top five based on either global force-displacement or local strain predictions, according to the lead SFC3 article by Kramer et al. (2019). One important conclusion from the student predictions is that thorough calibration of the elastic-plastic constitutive model (prior to onset of fracture/damage) seemed to be as important as, if not more important than, the fracture model, given that the specimens experienced a significant amount of plastic deformation prior to onset of fracture.

Based on the students' experiences participating in the SFC3 as a class project, advantages and disadvantages were identified for all three simulation approaches. Adaptive remeshing (performed using FRANC3D and Abaqus/Standard® version 6.14) exhibited the least mesh sensitivity by allowing for completely arbitrary crack propagation. However, it was the most computationally intensive of the approaches, especially when material-state mapping was employed. Two R-curve-calibration approaches were proposed for using adaptive remeshing without material-state mapping; one of which yielded promising results and should be explored further. XFEM (performed using Abaqus/Standard® version 6.14) exhibited mesh sensitivity and required much practice to generate appropriate meshes that would accommodate fracture in the challenge geometry. However, once an appropriate mesh was generated, XFEM seamlessly handled the plasticity-to-fracture transition. Element deletion (performed using Abaqus/Explicit® version 6.14) exhibited significant mesh sensitivity. However, it had the shallowest learning curve and seemed to be a suitable



option for beginning practitioners of computational fracture mechanics (although, it should be noted that the method does not technically predict the evolution of fracture surfaces based on fracture mechanics).

From a management and organizational standpoint, recommendations are offered for future classroom participation in the SFC or similar round-robin activities. In general, the recommendations are related to ensuring that classroom participation is tractable for a project of this magnitude and that focus remains on meeting the course learning objectives. The recommendations for faculty advisors include actively assisting students with tasks that do not directly meet the course learning objectives, controlling the rate and influx of information so students are not overwhelmed to the point of inaction, discussing with students what information or

data can be neglected in light of the course objectives, and setting clear and intermediate deliverables throughout the semester that allow students to tackle individual tasks on their way to meeting the final goal.

**Acknowledgements** A.D. Spear would like to acknowledge Professors Anthony Ingraffea and Alan Zehnder from Cornell University for inspiring the content and structure of the Fatigue and Fracture course. A.D. Spear's time on this project spent outside of the regular course obligations was supported by the National Science Foundation Faculty Early Career Award under Grant No. CMMI-1752400.

# **Appendix**

See Fig. 17.



Lecture	Date	Торіс	Description	1	
1	M: Jan. 9	Introduction	Administrative items; intro. to/history of fracture mechanics		Ī
2	W: Jan. 11	Crack-driving forces: energy approach	Energy balance and energy release rate (G)		١
	M: Jan. 16		MLK Jr. Day (no class)	nics	Linear Elastic Fracture Mechanics
3	W: Jan. 18	Crack-driving forces: stress approach	Stress fields and stress intensity factors (K)	cha	
4	M: Jan. 23	Crack-driving forces: stress approach	Crack-tip displacement fields; relationship between K & G	. Me	
5	W: Jan. 25	Crack-resisting forces	Fracture toughness, toughness testing (experimental methods) lab	ture	
6	M: Jan. 30	Crack-resisting forces	Crack stability, R-curves	Frac	
7	W: Feb. 1	Predicting crack growth	Computational fracture mechanics	stic	
8	M: Feb. 6	Predicting crack growth	Computational fracture mechanics (FE-based method)	· Ela	
9	W: Feb. 8	Predicting crack growth	Mixed-mode crack growth	near	
10	M: Feb. 13	Predicting crack growth	Mixed-mode crack growth	Ē	
11	W: Feb. 15	(Flex lecture)	LEFM Review, Discuss final projects		
	M: Feb. 20		Presidents' Day (no class)		
12	W: Feb. 22	Generalized (nonlinear) fracture parameters	Intro. to generalized (nonlinear) fracture mechanics, J-integral	nice	1100
	M: Feb. 27	EXAM 1 (Topic	cs in Linear Elastic Fracture Mechanics)	Generalized (Nonlinear) Fracture Mechanics	CHE
13	W: Mar. 1	Generalized (nonlinear) fracture parameters			
14	M: Mar. 6	Generalized (nonlinear) fracture parameters  J-integral (experimental determination)  Generalized (nonlinear) fracture parameters  J-integral (FEA determination)			T T
15	W: Mar. 8			[7	1 1 4
	M: Mar. 13	Spring Break (no class)			
	W: Mar. 15	Spring Break (no class)			
16	M: Mar. 20	Intro. to fatigue; Total-life approaches	Intro. to fatigue and fatigue design philosophies; Stress-life approach		
17	W: Mar. 22	Intro. to fatigue; Total-life approaches Intro. to fatigue and fatigue design philosophies; Stress-life approach			
18	M: Mar. 27	Damage-tolerance approach	LEFM-based approach to fatigue	an	
19	W: Mar. 29	7 Damage-tolerance approach LEFM-based approach to fatigue		Fatigue	
20	M: Apr. 3	Residual stresses	Effects and analysis of residual stresses	<u></u>	
21	W: Apr. 5	Materials science perspective on fatigue	Material deformation, micromechanics of crack nucleation, Stage I/II		
22	M: Apr. 10	(Flex lecture)	NLFM and Fatigue Review		
	W: Apr. 12	EXAM 2 (Topics in Nonlinear Fracture Mechanics and Fatigue)			_
23	M: Apr. 17	Fractography	Post-mortem characterization of failure surfaces	cial	Ī
24	W: Apr. 19	Guest lecturer from Composites Lab	Fracture and delamination in composite materials	Special Topics	
25	M: Apr. 24	Course content review and debriefing			_
	T.: May 2	FINAL PROJECT & P	RESENTATION DUE (3:30pm, Submit in Class)		

Fig. 17 Lecture-by-lecture schedule of the Fatigue and Fracture course offered at the University of Utah in the spring semester of 2017

### References

Abaqus V (2014) 6.14 Documentation. Dassault Systemes Simulia Corporation, 651

Boyce BL, Kramer SLB, Fang HE et al (2014) The Sandia Fracture Challenge: blind round robin predictions of ductile tearing. Int J Fract 186(1-2):5-68

Boyce BL, Kramer SLB, Bosiljevac TR et al (2016) The second Sandia Fracture Challenge: predictions of ductile failure under quasi-static and moderate-rate dynamic loading. Int J Fract 198(1–2):5–100

Erdogan F, Sih G (1963) On the crack extension of plates under plane loading and transverse shear. J Basic Eng 85(4):519–527

Ingraffea AR (2007) Computational fracture mechanics. In: Stein E, Borst R, Hughes TJR (eds) Encyclopedia of computational mechanics, vol 2. Wiley, Chichester, pp 375–402

Kramer SLB et al (2019) The third Sandia Fracture Challenge: predictions of ductile fracture in additively manufactured metal. Int J Fract. https://doi.org/10.1007/s10704-019-00361-1



Lan W, Deng X, Sutton M (2007) Three-dimensional finite element simulations of mixed-mode stable tearing crack growth experiments. Eng Fract Mech 74(16):2498–2517

- Lee HC, Choi JS, Jung KH, Im YT (2009) Application of element deletion method for numerical analyses of cracking. J Ach Mater Manuf Eng 35(2):154–161
- Mohammadi S (2008) Extended finite element method for fracture analysis of structures. Blackwell Publishing, Hoboken
- Moës N, Dolbow J, Belytschko T (1999) A finite element method for crack growth without remeshing. Int J Numer Methods Eng 46(1):131–150
- Pommier S (2011) Extended finite element method for crack propagation. Wiley, Hoboken
- Song JH, Kim DJ, Lee SH, Belytschko T (2008) A comparative study on dynamic fracture with finite element methods. In: 8th world congress on computational mechanics. Venice, Italy
- Spear AD, Priest AR, Veilleux MG, Hochhalter JD, Ingraffea AR (2011) Surrogate modeling of high-fidelity fracture simulations for real-time residual strength predictions. AIAA J 49(12):2770–782

- Sukumar N, Moës N, Moran B, Belytschko T (2000) Extended finite element method for three-dimensional crack modelling. Int J Numer Meth Eng 48:1549–1570
- Sutton M, Yan J, Deng X, Cheng C, Zavattieri P (2007) Threedimensional digital image correlation to quantify deformation and crack-opening displacement in ductile aluminum under mixed-mode I/III loading. Opt Eng 46(5):051003
- Wawrzynek PA, Carter BJ, Ingraffea AR (2009) Advances in simulation of arbitrary 3D crack growth using FRANC3D/NG.
  In: 12th international conference on fracture. Ottawa, Canada

**Publisher's Note** Springer Nature remains neutral with regard to jurisdictional claims in published maps and institutional affiliations.

